HHS Public Access

Author manuscript

Exp Hematol. Author manuscript; available in PMC 2022 July 05.

Published in final edited form as:

Exp Hematol. 2022 July ; 111: 66–78. doi:10.1016/j.exphem.2022.04.005.

Downregulation of SATB1 by miRNAs reduces megakaryocyte/erythroid progenitor expansion in preclinical models of Diamond–Blackfan anemia

Mark C. Wilkes[a], **Vanessa Scanlon**[b], **Aya Shibuya**[a], **Alma-Martina Cepika**[c], **Ascia Eskin**[d], **Zugen Chen**[d], **Anupama Narla**[a], **Bert Glader**[a], **Maria Grazia Roncarolo**[c], **Stanley F. Nelson**[d], **Kathleen M. Sakamoto**[a]

[a]Division of Hematology/Oncology, Department of Pediatrics, Stanford University, Stanford, CA;

[b]Yale Stem Cell Center, Department of Pathology, Yale School of Medicine, Yale University, New Haven, CT;

[c]Institute for Stem Cell Biology and Regenerative Medicine, Department of Genetics, Stanford University School of Medicine, Stanford, CA;

[d]Department of Pathology and Laboratory Medicine¸ David Geffen School of Medicine, University of California, Los Angeles, Los Angeles, CA

Abstract

Diamond−Blackfan Anemia (DBA) is an inherited bone marrow failure syndrome that is associated with anemia, congenital anomalies, and cancer predisposition. It is categorized as a ribosomopathy, because more than 80% or patients have haploinsufficiency of either a small or large subunit-associated ribosomal protein (RP). The erythroid pathology is due predominantly to a block and delay in early committed erythropoiesis with reduced megakaryocyte/erythroid progenitors (MEPs). To understand the molecular pathways leading to pathogenesis of DBA, we performed RNA sequencing on mRNA and miRNA from RPS19-deficient human hematopoietic stem and progenitor cells (HSPCs) and compared existing database documenting transcript fluctuations across stages of early normal erythropoiesis. We determined the chromatin regulator, SATB1 was prematurely downregulated through the coordinated action of upregulated miR-34 and miR-30 during differentiation in ribosomal insufficiency. Restoration of SATB1 rescued MEP expansion, leading to a modest improvement in erythroid and megakaryocyte expansion in RPS19 insufficiency. However, SATB1 expression did not affect expansion of committed erythroid progenitors, indicating ribosomal insufficiency affects multiple stages during erythroid differentiation.

Offprint requests to: Kathleen M. Sakamoto, Division of Hematology/Oncology, Department of Pediatrics, Stanford University, Stanford, CA 94305; kmsakamo@stanford.edu.

Conflict of interest disclosure

The authors have no competing interests to declare.

SUPPLEMENTARY MATERIALS

Supplementary material associated with this article can be found in the online version at https://doi.org/10.1016/j.exphem.2022.04.005.

Diamond−Blackfan Anemia (DBA) is a rare congenital bone marrow failure syndrome (estimated incidence of seven cases per million live births) with more than 90% of the reported cases presenting by 1 year of age. It is characterized by a macrocytic, moderate to severe anemia in association with hypoplastic bone marrow and reticulocy-topenia. Almost half of DBA patients exhibit physical abnormalities, including short stature, craniofacial anomalies (50% of patients), upper limb and hand—in particular thumb (38%) abnormalities and genitourinary (39%) as well as cardiac (30%) abnormalities [1]. DBA patients have an elevated predisposition for cancer, with the most common malignancies being myelodysplastic syndromes (MDS), acute myeloid leukemia (AML), colon carcinoma, osteosarcoma, and genitourinary cancers [2–5].

It remains unclear if DBA is caused by a hematopoietic defect at a single stage of differentiation, defects in multiple stages, or a general delay in differentiation. Evidence supports a block between the earliest committed erythroid progenitors and blast-forming unit–erythroid (BFU-E) stage [6] and the BFU-E and colony-forming unit–erythroid (CFU-E) stages of erythroid development [7]. However, a decrease in uncommitted hematopoietic progenitors has also been reported, with long-term bone marrow culture assays indicating defects in megakaryocytic and granulocytic progenitors [8,9] and, in rare cases of DBA, progression to complete aplasia [2]. Bone marrow aspirates and biopsies from DBA patients exhibiting severe erythroblastopenia with less common neutropenia and thrombocytopenia, and in rare instances thrombocytosis, have been described at diagnosis or during DBA evolution [1].

Defects in ribosome biogenesis have been reported in the pathogenesis of several inherited bone marrow failure syndromes, including DBA, Shwachman–Diamond syndrome, and dyskeratosis congenital [10]. Monogenic mutations in one of 22 genes encoding large or small subunit ribosomal protein genes clinically manifest as DBA. *RPS19* mutations are most common and account for more than 25% of cases [11]. Transduction of shRNA targeting RPS19 lentiviral constructs in human $CD34^+$ hematopoietic stem and progenitor cells (HSPCs) recapitulates disease pathogenesis in vitro, causing severe defects in erythropoiesis and modest reductions in other myeloid lineages [12–14].

The mechanistic link between ribosome insufficiency and erythroid failure is not fully understood but increased p53 stability contributes to DBA pathology [1,15–19]. p53 stabilization occurs in the erythroid lineage and is not ubiquitous [19]. Deregulation of the transcription factor, GATA1, is also linked to DBA [20,21] but a relationship between p53 and GATA1 deregulation in DBA has not been identified. Indeed, the mechanisms and key factors leading to DBA pathogenesis remain incompletely characterized.

SATB1 binds nucleosome-dense AT-rich regions of DNA [22] to modulate the chromatin landscape. Large loops in chromatin are induced through dimerization/tetramerization of chromatin-bound SATB1 [23], facilitating transcriptional and epigenetic changes that lead to rapid phenotypic transitions [24]. SATB1 expression is highest in thymic lymphocytes and pre-B cells [25] but is implicated in diverse cellular processes including embryonic stem cell differentiation [26], X-Chromosome inactivation [27], cortical development [28], epidermal differentiation [29], and breast cancer development [30]. It has been previously

reported that SATB1 expression is critical in early hematopoiesis. In humans, SATB1 controls the expansion of common myeloid progenitors (CMPs) by regulating expression of the master myeloid transcription factor Pu.1 [31–34]. In mouse hematopoiesis, Satb1 expression negatively influences differentiation along the myeloid lineage [35,36].

MicroRNAs (miRNAs) consist of 21–24 bases and are involved in regulation of posttranscriptional gene regulation and RNA silencing. Most miRNAs exert an inhibitory effect through binding of a short (6–8 nucleotide) sequence in the 3′ untranslated region (3′UTR) of a target mRNA, and binding is facilitated by a complementary sequence (seed sequence) in the miRNA [37]. MicroRNA expression is often very tissue specific [38], and the specific deregulation of miRNAs in the differentiation of erythroid progenitors during ribosome insufficiency has not been examined.

Here we report, in both preclinical models and DBA patient samples, that SATB1 is downregulated and the miRNAs miR-30 and miR-34 are upregulated. Furthermore, the downregulation of SATB1 is dependent on the binding of both miRNAs to the SATB1 3′UTR. Our data indicate erythroid-restricted upregulation of miR-30 accompanies p53 stabilization-induced miR-34 induction, which appears more ubiquitous in ribosomal insufficiency. We propose the requirement of both miRNAs to downregulate SATB1 contributes to the predominantly erythroid-specific effects of ribosome insufficiency.

EXPERIMENTAL PROCEDURES

Cell culture

Primary human $CD34^+$ hematopoietic stem and progenitor cells were purified from cord or peripheral blood (New York Blood Center, New York, NY) or from human fetal liver tissue (Advanced Bioscience Resources and University of California, Los Angeles Center for AIDS Research, Los Angeles, CA) using magnetic-activated cell sorting (Miltenyi Biotec, Bergisch Gladbach, North Rhine-Westphalia, Germany) and were cryopreserved. On thawing, cells were cultured in the erythropoiesis-promoting medium x-Vivo15 medium (Lonza, Basel, Switzerland) containing 10% fetal bovine serum, interleukin (IL)-3 (20 ng/mL), IL-6 (20 ng/mL), stem cell factor (50 ng/mL), and erythropoietin (3 U/mL), or in the hematopoiesis-promoting medium containing erythropoiesis medium + GM-CSF (20 ng/mL), thrombopoietin (50 ng/mL), and transferrin (1 mg/mL). Lymphoblastoid cell lines (LCLs) were cultured in Dulbecco's modified Eagle's medium (DMEM) supplemented with 10% fetal bovine serum. Stable cell lines expressing shRNA against RPS19 were generated by co-transfecting shRNA-carrying vectors (pLVTH) with neomycin-carrying vector (pcDNA3.1) using Lipofectamine 2000 (Thermo Fisher). Individual clones were harvested and expanded in 100 μg/mL neomycin, and RPS19 expression was examined by Western blot and quantitative reverse transcription polymerase chain reaction (qRT-PCR).

Lentiviral transduction

Primary $CD34^+$ cells were transduced as published [12] with lentivirus expressing short hairpin RNA (shRNA) against RPS19, p53, SATB1, or luciferase (Luc), siRNA against SATB1 or a non-targeting (NT) sequence, or complementary DNA (cDNA) expressing

SATB1 or luciferase genes fused with wild-type 3′UTR, or a mutated 3′UTR. Virus co-expressed GFP, RFP, mCherry, or puromycin to enable selection.

Colony assays

Sorted hematopoietic cells were seeded in methylcellulose medium containing IL-3, stem cell factor, granulocyte−macrophage colony-stimulating factor, and erythropoietin (H4434; STEMCELL Technologies, Vancouver, BC, Canada) in triplicate, with 1,000 cells per plate. Erythroid (burst-forming unit erythroid) and myeloid (colony-forming unit, granulocyte–macrophage) colonies were counted 14–18 days later. In some cases, 3,000 cells per plate were added to ensure enough colonies for robust statistical analysis.

Flow cytometry

For cell surface flow cytometry, cells were incubated with human Fc receptor binding inhibitor (No. 14-9161-73, eBioscience, San Diego, CA) followed by primary antibodies CD235-APC (No. 306607, BioLegend, San Diego, CA), CD41-FITC (RRID: AB_314373, BioLegend No. 303703), and CD11b-PE/Cy5 (No. 101209, RRID: AB_312995, BioLegend) or CD-71-APC (No. BD551374, RRID: AB_398500, BD Biosciences, Franklin Lakes, NJ), CD34-Fluor450 (No. 48-0341-82, RRID: AB_468936, eBioscience), CD34-PE/Cy7 (No. 343615, RRID: AB_2629725, BioLegend), and GATA1-PE (No. 13353, RRID: AB_2798187, Cell Signaling Technology, Danvers, MA). Data were collected on a DxP10 flow cytometer (Cytek, Cerritos, CA) and analyzed using FlowJo Software, Version 9.7.2.

Quantitative reverse transcription polymerase chain reaction

RNA was extracted by using total RNA mini kit (Bio-Rad). RNA was transcribed into cDNA by using the iScript cDNA Synthesis Kit (Bio-Rad). Quantitative RT-PCR was run with iQ SYBR Green MasterMix (Bio-Rad, Hercules, CA) using the CFX384 Touch Real-Time PCR Detection System (Bio-Rad). 7SL small cytoplasmic RNA [12] was used as an internal control. Mitochondrial RNA was quantified using TaqMan Small RNA Assays (Applied Biosystems, Waltham, MA) per manufacturer's directions and normalized to snoRNA. Fold change of mRNA and miRNA was calculated using the comparative C_t method.

Luciferase assay

The SATB1 3′UTR (1885 3′ nucleotides) were cloned upstream, or downstream respectively, of firefly luciferase in pLenti-GIII-CMV-RFP-2A-Puro (abm) and transduced into $CD34^+$ cord blood progenitors that were differentiated in 1 μg/mL puromycin for 6 days. Transduction efficiency was normalized by RFP expression, and firefly luciferase activity determined by Luciferase Assay Reagent II (LAR II) from Dual-Luciferase Reporter (DLR) Assay System (Promega, Madison, WI). Luminescence was assessed using a Synergy H1 hybrid multimode microplate reader (BioTek, Winooski, VT).

Western blotting

Antibodies against RPS19 (Abcam No. AB40833, RRID AB_777759, 1:200 dilution, Abcam, Cambridge, UK), SATB1 (Abcam No. 49061, RRID: AB_882454,1:500 dilution), GATA1 (Cell Signaling No. 3535, RRID: AB_2108288, 1:500 dilution) HSP70 (Cell

Signaling No. 4873, RRID: AB_2119694, 1:1000 dilution), and GAPDH (Millipore No. MAB374, RRID: AB_2107445,1:10,000, Millipore, Burlington, MA) were used according to the manufacturer's instructions. The target proteins were analyzed by using SuperSignal West Pico Chemiluminescent Substrate for horseradish peroxidase (Thermo Fisher Scientific, Waltham, MA). Densitometry was performed using ImageJ software (http://rsb.info.nih.gov/ij/). When indicated, proteins were co-immunoprecipitated before immunoblotting. Cell lysates were normalized for protein before preclearing with Upstate Protein A/G Agarose for 30 min, before incubating with indicated antibody overnight. Immune complexes were precipitated with Protein A/G Agarose and separated by sodium dodecyl sulfate–polyacrylamide gel electrophoresis (SDS-PAGE), before being subjected to immunoblotting.

Cloning and CRISPR/Cas9

Lentiviral constructs expressing SATB1 cDNA, SATB1 and luciferase cDNA with various 3′UTR mutants were generated with standard molecular biology techniques.

Normalization and statistics

Hematopoietic lineage populations were normalized across replicates and experiments. Raw data and calculations performed to generate displayed plots are provided in the Supplementary Data (online only, available at www.exphem.org). The p values for statistical significance were obtained by using a paired Student t test. Significance was designated at $p \leq 0.05$. The data are representative of at least three independent experiments.

Resource availability

Lead contact.—Further information and requests for resources and reagents should be directed to and will be fulfilled by the Lead Contact, Kathleen Sakamoto (kmsakamo@stanford.edu).

Material availability.—Reagents generated in this study will be made available on request, but we may require a payment and/or a completed Materials Transfer Agreement if there is potential for commercial application.

Data and code availability.—This study did not generate/analyze code.

RESULTS

Identification of SATB1 as master regulator of early erythroid genes in RPS19-insufficient HSPCs

In DBA, ribosomal insufficiency is germline but manifests primarily as a defect in early erythropoiesis [1]. To understand the molecular pathways contributing to anemia in DBA, we performed RNA-seq on differentiated human fetal liver $CD34^+$ hematopoietic stem and progenitor cells (HSPCs) in which RPS19 expression had been suppressed by approximately 50% through transduction with shRNA. For comparison, HSPCs were transduced with shRNA against luciferase. As many of the differentially expressed genes may be shared by multiple cell types or play no role in the earliest stages of erythropoiesis where

ribosome insufficiency acts, we attempted to enrich for early erythropoiesis-specific genes by comparing our results with a publicly available RNA-seq data set analyzing differentially transcribed genes between human $CD34^+$ HSPCs and early burst-forming unit-erythroid (BFU-E) colony-forming progenitors [39]. Forty-two genes identified in both data sets were defined as RPS19 insufficiency-sensitive early erythroid genes (Figure 1A). Our initial screen was performed in fetal liver cells, but because DBA does not manifest until infancy, we also compared RPS19 insufficient with control in differentiating HSPCs derived from cord blood. Transcript copy numbers of the 42 RPS19-sensitive early erythroid genes from HSPC populations from cord blood and fetal liver at days 0 and 5 were evaluated by qPCR and defined as upregulated, downregulated or no change. RPS19-Insufficient samples could also be further categorized as “further” up- or downregulated, relative to controls (Figure 1B).

MicroRNA sequencing data comparing microRNAs from RPS19-insufficient and control HSPCs identified the most significantly upregulated miRNAs (>1.8-fold) in RPS19-insufficient HSPCs including miR-34a, -b, and -c, as well as miR-30 ($p = 0.004$, 0.0082, 0.0232 and 0.0085) (Figure 1C). The 3′UTRs of 6 of the 42 RPS19-sensitive erythroid genes, including SATB1, contained putative binding sequences for miR-34 and/or miR-30 (Figure 1D). Of these 6, SATB1 has binding sequences for both miR-34 and miR-30 and led us to focus on the role of SATB1 and miRNA deregulation in the pathogenesis of DBA.

SATB1 mRNA is ordinarily downregulated during normal erythropoiesis [39,40] but our RNA-seq analysis of RPS19-insufficient HSPCs suggests SATB1 mRNA is significantly lower than in control HSPCs (2.6 times, $p = 0.0361$; Figure 1B). This was confirmed by qRT-PCR, with SATB1 mRNA reduced by 22% in control cultures, but 62% lower in RPS19 insufficiency after 5 days (Figure 1E). This indicates a 2.8-fold increased downregulation ($p = 0.0202$). Western blot analysis revealed a similar reduction in protein expression (Figure 1F). Downregulation of SATB1 mRNA in MEPs and proerythroblasts has also recently been reported in a transcriptomic analysis of DBA patients with RPS19 and CECR1 mutations [41].

To ensure SATB1 and miR-30/34 deregulation was not due to a sequence-specific artifact of the shRNA, we transduced three separate RPS19 shRNAs into Kp53A1 and $CD34^+$ HSPCs. After 3 days, RPS19 expression was reduced 35.3%, 59.6%, and 77.3% in Kp53A1 cells and 28.3%, 56%, and 77% after 5 days in differentiating HSPCs (Supplementary Figure E1A, upper panels, online only, available at www.exphem.org). SATB1 expression was reduced 29.8%, 35.2%, and 45.7% in Kp53A1s and 46.7%, 60.3%, and 75.8% in HSPCs (Supplementary Figure E1A, lower panels, online only, available at www.exphem.org). Expression of both miR-30 and miR-34 increased in RPS19 insufficiency, irrespective of the shRNA sequence, with the increase in expression inversely correlated to both RPS19 and SATB1 expression (Supplementary Figure E1A, middle panels, online only, available at www.exphem.org).

To examine SATB1 deregulation in hematopoiesis in DBA patients, we derived iPSCs from a DBA patient with an RPS26 mutation and healthy control, before differentiating them to $CD34^+$ HSCs as previously described [42]. The control clones were transduced with a

tetracycline-inducible shRNA against RPS19, while the DBA clones were transduced with a tetracycline-inducible wild-type RPS26 and differentiated for 5 days. Compared with untreated controls, expression of shRPS19 and the untreated DBA clones reduced SATB1 expression to 31.4% ($p = 0.0013$) and 46.9% ($p = 0.0014$), respectively. Re-expression of RPS26 in the DBA clones increased expression of SATB1 from 46.9% to 83.4% ($p = 0.0103$) of healthy controls (Figure 1G, top). RPS19, RPS26, and GAPDH protein expression was determined by Western blot analysis (Figure 1G, bottom).

SATB1 re-expression modestly restores erythropoiesis in RPS19 insufficiency

To determine if loss of SATB1 drives erythropoiesis failure in ribosomal insufficiency, we transduced cord blood (CB) $CD34^+$ HSPCs with lentivirus expressing shRNA against RPS19 (resulting in 50% knockdown) in the presence or absence of transduced SATB1 cDNA. Contrary to our hypothesis, re-expression of SATB1 in RPS19-insufficient progenitors did not improve erythroid (BFU-E) colony formation (from 19.1% to 20.1% of controls, $p = 0.7374$) (Figure 2A). However, re-expression of SATB1 significantly rescued CFU-GM colony formation ($p = 0.0397$) from 74.8% to 98% of control (Figure 2B). Interestingly, while the number of BFU-E colonies was not substantially increased, several of the colonies were orders of magnitude larger than observed in RPS19 insufficiency or controls (Figure 2C). Images of representative plates (Figure 2C, left) and BFU-E colonies (Figure 2C, right) are provided. Analysis of cell composition after dissolution of the methylcellulose indicated that restoration of SATB1 modestly rescued $CD235^+$ expansion ($p = 0.0045$) from 16% to 44% of healthy controls (Figure 2D).

In liquid culture of RPS19-insufficient progenitors, SATB1 restoration did not increase $CD235^+$ expansion to the same extent as observed in methylcellulose (Figure 2E, top), but remained statistically significant (1.9-fold, $p = 0.0202$). A mild increase of 10.2% in $CD11b^+$ expansion ($p = 0.0445$) was also observed (Figure 2E, middle). Most strikingly, RPS19-insufficient $CD41^+$ megakaryocytes expressing recombinant SATB1 expanded more than twofold above healthy controls (Figure 2E, bottom). Protein expression of SATB1, RPS19, and GAPDH in differentiating HSPC populations at days 0 and 5 is illustrated in Supplementary Figure E2 (online only, available at www.exphem.org).

Extensive data suggest erythropoietic defects in DBA manifest primarily in the earliest committed erythroid progenitors. As SATB1 re-expression did not dramatically rescue erythropoiesis, the loss of SATB1 is not the only mechanism leading to the severe erythroid-specific defects of DBA, especially as SATB1 re-expression did not exclusively affect the erythroid lineage. Finally, although SATB1 is prematurely downregulated in RPS19 insufficiency, SATB1 expression is gradually reduced during normal erythropoiesis and is largely absent by committed erythropoiesis (Figure 1F) [11]. As SATB1 re-expression both increases erythropoiesis and fully rescues RPS19 insufficiency of other myeloid lineages, our data are consistent with the loss of SATB1 expression affecting the expansion of shared, non-committed myeloid progenitors. Indeed, a role for SATB1 has been established in primitive myeloid progenitor expansion [32].

Premature downregulation of SATB1 mediated by coordinated induction of miR-34 and miR-30 in RPS19 insufficiency

To understand the role of miRs in SATB1 regulation and erythropoiesis, we examined the effect of miR-34 and miR30 on SATB1 expression. The 3′UTR of SATB1 contains consensus sequences for the binding of miR-34 and miR-30 (Supplementary Figure E3A, online only, available at www.exphem.org). Both of these miRNAs were upregulated by RPS19 insufficiency (Figure 1C; Supplementary Figure E1, online only, available at www.exphem.org). Quantitative RT-PCR confirmed that RPS19 insufficiency induced miR-34 and miR-30 expression by 2.4-fold ($p = 0.0242$) and 3.2-fold ($p = 0.0306$), respectively, after 5 days of differentiation (Figure 3A, top). RPS19 expression was reduced to 40.3% of controls when transduced with shRNA against RPS19 (Figure 3A, bottom). Transfection of miR-30 or miR-34 individually into healthy HSPCs had a minimal effect on the reduction of endogenous SATB1 or the luciferase-SATB1 3′UTR construct, but when miR-30 and miR-34 were co-expressed, endogenous SATB1 expression was reduced to 36.4% ($p = 0.0058$) and luciferase-SATB1 3′UTR to 47.8 % ($p = 0.0174$) when compared with controls in which no miRNAs were expressed (Figure 3B).

Mutation of the two potential miRNA binding sites within the 3′UTR of SATB1 (see Figure 3C) revealed premature downregulation of SATB1 in RPS19 insufficiency is dependent on both miR-34 and miR-30 sites. Mutant, or wild-type, SATB1 3′UTRs were fused to the luciferase gene and transduced into differentiating HSPCs also expressing nontargeting (NT) or RPS19-targeted shRNA. Luciferase degradation was not observed when co-expressed with NT, irrespective of the wild type or mutant 3′UTR (Figure 3D, left). In RPS19-insufficient HSPCs, luciferase fused to the WT SATB1 3′UTR was rapidly degraded. In contrast, no degradation of luciferase transcripts was observed when both the miR-34 and miR-30 binding sites were mutated. Mutation of either predicted miRNA binding site alone resulted in minimal luciferase degradation (Figure 3D, right). Consensus sequences and mutations are illustrated in Supplementary Figure E3A (online only, available at www.exphem.org). This suggests that both miRNA binding sites are required for RPS19 insufficiency-induced SATB1 downregulation. Expression of luciferase-fused SATB1 3′UTRs did not affect the degradation of endogenous SATB1 in control or RPS19 insufficiency (Supplementary Figure E3B, online only, available at www.exphem.org). Endogenous SATB1 is downregulated gradually whereas expression of luciferase fused to the SATB1 3′UTR remained stable, indicating downregulation in normal erythropoiesis is not mediated by the 3′UTR.

Our data support the hypothesis that binding of miR-34 and miR-30 to the predicted binding sequences initiates SATB1 downregulation and indicate SATB1 is prematurely downregulated in RPS19-insufficient HSPCs through coordinated upregulation of miR-30 and -34.

Stabilized p53 induces miR-34, but not miR-30, in erythroblasts

Increased stability and activity of p53 in erythroid progenitors have previously been reported in DBA [1,12,18]. Although the majority of studies indicate increased p53 activity is restricted to erythroid progenitors, increased p53 has also been reported in DBA patient-

derived LCLs [43]. The upregulation of miR-34 in response to p53 upregulation is well characterized [44]; however, the expression of p53 and miR-30 has been reported to be either proportional to [45] or inversely proportional to [46,47] p53 expression. We observed that on transduction of shRNAs against both RPS19 and p53, miR-34 upregulation is decreased from 2.3- to 1.2-fold of control ($p = 0.0127$) (Figure 4A, left) while miR-30 upregulation persists (Figure 4A, middle). The enhanced downregulation of SATB1 also did not occur when p53 expression was suppressed (Figure 4A, right). Validation of RPS19 and p53 knockdown after lentiviral transduction is illustrated in Supplementary Figure E4 (online only, available at www.exphem.org).

DBA patient-derived LCLs averaged 1.9- and 2.2-fold increases in p53 protein and miR-34 expression, respectively, compared with healthy control, but no significant difference in miR-30. Expression of shRNA against RPS19 in the healthy control cells recapitulated the observations in DBA-derived samples (Figure 4B). This fits a model whereby ribosomal insufficiency induces p53 and miR-34 in many cell types, but the induction of miR-30 in RPS19 insufficiency is more restricted (Figure 4C).

SATB1 is a master regulator of RPS19-sensitive early erythroid genes

As SATB1 is a broad genome chromatin regulator [41], we hypothesized that SATB1 loss may contribute to dysregulation of some of the other 41 RPS19-sensitive early erythroid genes we identified in Figure 1. We transduced a lentiviral vector expressing the SATB1 cDNA in RPS19-insufficient HSPCs leading to a significant correction in the expression of 16 of the 41 genes and partial correction of 10 genes (Figure 5A). This is consistent with a role for SATB1 as a significant regulator of RPS19-sensitive early erythroid genes (Figure 5B).

Examination of the chromosomal localization of each of these genes indicates SATB1-influenced genes tend to be clustered in groups spanning less than 8 Mb, whereas genes not influenced by SATB1 are more uniformly distributed across the chromosomes (Figure 5C). Strikingly, in RPS19-insufficient HSPCs, inhibition of both miR-34 and miR-30 restored the regulated expression of the same 16 early erythroid genes that were sensitive to RPS19 insufficiency, and were rescued by restoration of SATB1 expression, while inhibition of either alone did not (Figure E5A, online only, available at www.exphem.org).

Similarly, suppression of miR-30 or miR-34 alone did not significantly rescue erythroid or myeloid populations, but, in combination, improved $CD235^+$ erythroid expansion by 1.5-fold ($p = 0.0453$) (Supplementary Figure E5B, top, online only, available at www.exphem.org), $CD11b^+$ myeloid expansion by 1.1-fold ($p = 0.0237$) (Supplementary Figure E5B, middle, online only, available at www.exphem.org), and $CD41^+$ megakaryocyte expansion by 2.1-fold ($p = 0.0141$) (Supplementary Figure E5B, bottom, online only, available at www.exphem.org). For comparison, SATB1 re-expression increased erythroid, myeloid, and megakaryocyte expansion by 1.9-, 1.1-, and 2.3-fold respectively (Figure 2E).

SATB1 downregulation contributes to DBA pathogenesis by reducing MEP expansion

As expected, SATB1 expression was reduced by 26.4% ($p = 0.0052$) in normal $Lin^-CD34^+CD38^{mid}CD45RA^-FLT3^-MPL^+CD36^-CD41^-$ MEPs compared with

Lin^{-}CD34^{+}CD38^{+}CD45RA^{-}FLT3^{+}MPL^{+} CD36^{-}CD41^{-} CMPs (Figure 6A). RPS19 insufficiency further downregulated SATB1 expression in both CMPs and MEPs. RPS19-Insufficient CMPs expressed 86.1% ($p = 0.0332$) of control CMPs, whereas RPS19-insufficient MEPs expressed 49.2% ($p = 0.0053$) of control MEPs (Figure 6A). A similar downregulation of SATB1 in MEPs of DBA patients has been reported [42], indicating the SATB1 downregulation in in vitro RPS19 insufficiency faithfully recapitulates DBA in patients.

To examine our hypothesis that premature SATB1 downregulation contributes to the reduction in erythropoiesis by reducing MEP expansion, we isolated enriched Lin^{-}CD34^{+}CD38^{+}CD45RA^{-}FLT3^{+}MPL^{+}CD36^{-}CD41^{-} CMP population from CB CD34^{+} HSPCs and transduced with shRNA against RPS19 or control and tetracycline-inducible SATB1 cDNA. Cultures were differentiated for 4 days before assessment of Lin^{-}CD34^{+}CD38^{mid} CD45RA^{-}FLT3^{-}MPL^{+}CD36^{-}CD41^{-} MEPs. RPS19-Insufficient cultures exhibited a reduction in MEPs by 28.9% ($p = 0.0055$) compared with controls. This was rescued by SATB1 re-expression and was statistically indistinguishable ($p = 0.1364$) from controls (Figure 6B).

To determine if SATB1 deregulation contributed to erythroid defects in more differentiated progenitors, Lin^{-}CD34^{+}CD38^{mid}CD45RA^{-}FLT3^{-}MPL^{+}CD36^{-}CD41^{-} MEPs were isolated and transduced with shRNA against RPS19 or control and tetracycline-inducible SATB1 cDNA. After 10 days, CD235^{+} erythrocytes were reduced by 68.4% relative to controls ($p = 0.0008$), and the re-expression of SATB1 did not significantly ($p = 0.3$) influence erythropoiesis. CD41a^{+} megakaryocyte expansion was not significantly influenced by RPS19 ($p = 0.3902$) or SATB1 ($p = 0.3478$) levels (Figure 6C).

Collectively we report that SATB1 is downregulated during RPS19 insufficiency, and this is mediated by the upregulation of miR-30 and miR-34. While miR-34 upregulation is downstream of p53 stabilization, miR-30 induction is p53 independent. We argue the consequence of SATB1 downregulation in the disruption of erythropoiesis in DBA is a modest reduction in the expansion of MEPs, but the biology of more differentiated progenitors may also be affected through deregulation of SATB1-regulated early erythropoiesis genes.

DISCUSSION

This study is the first to describe a role for SATB1 in DBA pathogenesis and erythropoiesis. On the basis of our data, we propose an aberrant multistep pathway that is initiated in early myeloid progenitors. In early, non-committed myeloid progenitors, RPS19 insufficiency induces p53 and miR-30 upregulation. Increased p53 upregulates miR-34, which cooperates with miR-30 to downregulate SATB1. Although many transcriptomic studies compare mRNA from more mature erythroid progenitors (where SATB1 expression is already low) a study examining HSCs, MEPs, and proerythroblasts from DBA patients with RPS19 and CECR1 mutations similarly observed a significant downregulation of SATB1 in DBA MEPs [42].

The loss of SATB1 deregulates a number of RPS19-sensitive early erythroid genes and reduces expansion of MEP (and, to a lesser extent, CMP) progenitors. RPS19 insufficiency manifests an additional, more robust blockage later in early committed erythroid progenitors that is largely independent of SATB1. Our study has focused on erythroid expansion as a readout of erythropoiesis, but it remains possible that erythroid transcripts deregulated by SATB1 downregulation may contribute to aberrant function, development, or localization of more mature erythroid cells. A number of the SATB1-regulated proteins identified in Figure 5 can affect cellular activities at later stages of erythropoiesis [43]. Figure 7 is a schematic of erythroid differentiation under conditions of RPS19 and SATB1 modulation that best represents the results of our study.

It should be noted that in healthy erythropoiesis, SATB1 expression is highest in HSCs and is gradually reduced as uncommitted progenitors differentiate, becoming very low once cells commit to erythropoiesis. In these cells, all myeloid lineages expand normally (Fig 7, top left). RPS19 insufficiency suppresses SATB1 expression to reduce MEP expansion, but also induces SATB1-independent events that cause additional severe defects in committed erythroid progenitors. This yields a severe reduction in $CD235^{+}$ erythrocytes (Figure 7, top right). Re-expression of SATB1 in RPS19 insufficiency corrects the deficiencies in nonerythroid myeloid lineages, but does not substantially rescue the severe, SATB1-independent defect in committed erythroid progenitors (Figure 7, bottom).

The failure to fully correct erythropoiesis with SATB1 re-expression in RPS19 insufficiency is due to SATB1-independent events occurring during committed erythropoiesis. This likely includes GATA1 regulatory defects, such as GATA1 transcript-specific translational sensitivity to reduced ribosome levels [20], and other events including NLK activation and tumor necrosis factor (TNF)-α induction [12].

Although heterozygous germline RPS19 mutations occur in all cells, it remains unclear why erythroid cells are most obviously affected. The upregulation and role of p53 in DBA and RPS19 insufficiency are well characterized [1,12,15,16,18,19] and have been reported to be restricted to erythroid cells [18]. However, as we and others [48] have observed p53 upregulation in LCLs generated from DBA patients, the erythroid specificity remains unclear. Similarly, the induction of miR-34 in response to increased p53 is firmly established [44]; however, p53 has been reported to induce miR-30 to inhibit colorectal cancer [47], but can also suppress p53, perhaps serving as a feedback loop [46,47]. Synergy between miR-30 and other miRNAs has been observed. MiR-30 and miR181 synergize to suppress p53 in diabetes-induced cardiac hypertrophy [46]. Coincidently, miR181 is upregulated in nonerythroid hematopoietic lineages [33], while in DBA, p53 upregulation is most prominent in the erythroid lineage [18]. Perhaps in DBA, in the absence of miR-181, miR-30 synergizes with miR-34 in erythroid progenitors to downregulate SATB1, while synergizing with miR-181 in other cells to counter RPS19-insufficiency-induced p53 stabilization.

An unexpected result was the dramatic increase in megakaryocyte expansion on SATB1 re-expression in RPS19 insufficiency. As ribosomal protein insufficiency has been determined to slow the progression of cells through each stage of differentiation [49], it is possible

that the re-expression of SATB1 maintains MEPs in a more proliferative state longer than normal. Generation of such MEP-like proliferative cells has been described previously [50].

It is also plausible that this delay in differentiation could be attributed to the unexpectedly large size and increased expansion of some BFU-E colonies on re-expression of SATB1. In this model, both early megakaryocytes and erythroid progenitors could have outproliferated controls, but the SATB1-independent RPS19 insufficiency would prevent further maturation of erythroblasts. The enlarged colonies may represent committed erythroid progenitors that "escaped" or are "resistant" to the downstream block and endured a prolonged transition through more proliferative stages. Indeed, this is one proposed mechanism of the action of corticosteroids steroids in DBA [51]. Steroids also improve expansion in later stages of erythropoiesis (BFU-E to CFU-E) where they have been determined to improve anemia until resistance develops [1].

Another possible explanation for enlarged BFU-E colonies may be a side effect of constitutive expression of recombinant SATB1 (endogenous SATB1 is gradually downregulated) that maintains SATB1 and SATB1-regulated erythroid genes later into erythropoiesis than observed in wild-type erythroblasts. Alternatively, the observed colonies may be enlarged because SATB1 expression influences RPS19-sensitive erythroid genes (Figure 5) that can affect later stages of erythropoiesis under stressed conditions that may not be uniform across agar plates [52]. It should be noted that more than 95% of colonies when SATB1 is re-expressed are of similar size to those without SATB1 re-expression, indicating heterogeneity in the phenotype.

The molecular mechanisms through which SATB1 regulates the RPS19-sensitive early erythroid genes has not been elucidated. As SATB1 can bind chromatin and form loops [23], one possible mechanism is that the presence of SATB1 may be required to spatially regulate transcriptional elements during early hematopoiesis. In this way, the loss of SATB1 expression during differentiation could disrupt the transcriptional program requiring the chromatin loops. Alternatively, SATB1 can bind histone deacetylases [53–55] and may regulate transcriptional activity through modulation of the chromatin histone signature. As a number of the identified SATB1-regulated RPS19-sensitive early erythroid genes are linked to DBA and other anemias, determining the regulatory mechanisms by which SATB1 modulates each of these genes may provide insight into the earliest steps of erythroid commitment that are disrupted in this disease.

Ribosomal insufficiency affecting erythropoiesis is well characterized in DBA, so on uncovering a loss of SATB1 in RPS19 insufficiency, it was not unexpected to find a role for SATB1 in erythropoiesis. But the SATB1 effect on nonerythroid expansion was unexpected. DBA is classically considered a pure red blood cell aplasia [1]; however, bone marrow aspirates and biopsies from DBA patients demonstrate severe erythroblastopenia with less common neutropenia and thrombocytopenia and, in rare instances, thrombocytosis [1]. DBA patients can present with neutropenia and thrombocytopenia intermittently throughout their lives [11], and we postulate that downregulation of SATB1 not only contributes to the erythroid defects, but may also be responsible for other hematological manifestations of the disease.

Supplementary Material

Refer to Web version on PubMed Central for supplementary material.

Acknowledgments

This work was funded by a National Institutes of Health (NIH) T32 Training Grant DK098132, K01 Early Career Development Grant K01DK123140), a Maternal Child Health Research Institute fellowship and K award support grant (to MCW), the Diamond Blackfan Anemia (DBA) Foundation, the Department of Defense (No. BM180024), the SPARK program at Stanford, and California Institute of Regenerative Medicine Grant DISC2-12474 (to KMS).

REFERENCES

1. Da Costa L, Narla A, Mohandas N. An update on the pathogenesis and diagnosis of Diamond–Blackfan anemia. F1000Res. 2018;7. F1000 Faculty Rev-1350.
2. Alter BP, Giri N, Savage SA. Rosenberg PS. Cancer in the National Cancer Institute inherited bone marrow failure syndrome cohort after fifteen years of follow-up. Haematologica 2018;103:30–9. [PubMed: 29051281]
3. Lipton JM, Federman N, Khabbaze Y, et al. Osteogenic sarcoma associated with Diamond–Blackfan anemia: a report from the Diamond–Blackfan Anemia Registry. J Pediatr Hematol Oncol 2001;23:39–44. [PubMed: 11196268]
4. Vlachos A, Rosenberg PS, Atsidaftos E, Alter BP, Lipton JM. Incidence of neoplasia in Diamond Blackfan anemia: a report from the Diamond Blackfan Anemia Registry. Blood 2012;119:3815–9. [PubMed: 22362038]
5. Vlachos A, Rosenberg PS, Atsidaftos E, et al. Increased risk of colon cancer and osteogenic sarcoma in Diamond–Blackfan anemia. Blood 2018;132:2205–8. [PubMed: 30266775]
6. Devlin EE, Dacosta L, Mohandas N, Elliott G, Bodine DM. A transgenic mouse model demonstrates a dominant negative effect of a point mutation in the RPS19 gene associated with Diamond–Blackfan anemia. Blood 2010;116:2826–35. [PubMed: 20606162]
7. Ohene-Abuakwa Y, Orfali KA, Marius C, Ball SE. Two-phase culture in Diamond Blackfan anemia: localization of erythroid defect. Blood 2005;105:838–46. [PubMed: 15238419]
8. Casadevall N, Croisille L, Auffray I, Tchernia G, Coulombel L. Age-related alterations in erythroid and granulopoietic progenitors in Diamond–Blackfan anaemia. Br J Haematol 1994;87:369–75. [PubMed: 7524624]
9. Santucci MA, Bagnara GP, Strippoli P, et al. Long-term bone marrow cultures in Diamond–Blackfan anemia reveal a defect of both granulomacrophage and erythroid progenitors. Exp Hematol 1999;27:9–18. [PubMed: 9923439]
10. Ganapathi KA, Shimamura A. Ribosomal dysfunction and inherited marrow failure. Br J Haematol 2008;141:376–87. [PubMed: 18410571]
11. Narla A, Vlachos A, Nathan DG. Diamond Blackfan anemia treatment: Past, present, and future. Semin Hematol 2011;48:117–23. [PubMed: 21435508]
12. Bibikova E, Youn MY, Danilova N, et al. TNF-mediated inflammation represses GATA1 and activates p38 MAP kinase in RPS19-deficient hematopoietic progenitors. Blood 2014;124:3791–8. [PubMed: 25270909]
13. Jaako P, Flygare J, Olsson K, et al. Mice with ribosomal protein S19 deficiency develop bone marrow failure and symptoms like patients with Diamond–Blackfan anemia. Blood 2011;118:6087–96. [PubMed: 21989989]
14. Miyake K, Flygare J, Kiefer T, et al. Development of cellular models for ribosomal protein S19 (RPS19)-deficient Diamond–Blackfan anemia using inducible expression of siRNA against RPS19. Mol Ther 2005;11:627–37. [PubMed: 15771965]
15. Danilova N, Sakamoto KM, Lin S. p53 family in development. Mech Dev 2008;125:919–31. [PubMed: 18835440]

16. Danilova N, Sakamoto KM, Lin S. Ribosomal protein S19 deficiency in zebrafish leads to developmental abnormalities and defective erythropoiesis through activation of p53 protein family. Blood 2008;112:5228–37. [PubMed: 18515656]
17. Danilova N, Sakamoto KM, Lin S. Ribosomal protein L11 mutation in zebrafish leads to haematopoietic and metabolic defects. Br J Haematol 2011;152:217–28. [PubMed: 21114664]
18. Dutt S, Narla A, Lin K, et al. Haploinsufficiency for ribosomal protein genes causes selective activation of p53 in human erythroid progenitor cells. Blood 2011;117:2567–76. [PubMed: 21068437]
19. Gazda HT, Sieff CA. Recent insights into the pathogenesis of Diamond-Blackfan anaemia. Br J Haematol 2006;135:149–57. [PubMed: 16942586]
20. Khajuria RK, Munschauer M, Ulirsch JC, et al. Ribosome levels selectively regulate translation and lineage commitment in human hematopoiesis. Cell 2018;173:90–103. e119. [PubMed: 29551269]
21. Ludwig LS, Gazda HT, Eng JC, et al. Altered translation of GATA1 in Diamond–Blackfan anemia. Nat Med 2014;20:748–53. [PubMed: 24952648]
22. Ghosh RP, Shi Q, Yang L, et al. Satb1 integrates DNA binding site geometry and torsional stress to differentially target nucleosome-dense regions. Nat Commun 2019;10:3221. [PubMed: 31324780]
23. Nakagomi K, Kohwi Y, Dickinson LA, Kohwi-Shigematsu T. A novel DNA-binding motif in the nuclear matrix attachment DNA-binding protein SATB1. Mol Cell Biol 1994;14:1852–60. [PubMed: 8114718]
24. Galande S, Purbey PK, Notani D, Kumar PP. The third dimension of gene regulation: Organization of dynamic chromatin loopscape by SATB1. Curr Opin Genet Dev 2007;17:408–14. [PubMed: 17913490]
25. Dickinson LA, Dickinson CD, Kohwi-Shigematsu T. An atypical homeodomain in SATB1 promotes specific recognition of the key structural element in a matrix attachment region. J Biol Chem 1997;272:11463–70. [PubMed: 9111059]
26. Savarese F, Davila A, Nechanitzky R, et al. Satb1 and Satb2 regulate embryonic stem cell differentiation and Nanog expression. Genes Dev 2009;23:2625–38. [PubMed: 19933152]
27. Agrelo R, Souabni A, Novatchkova M, et al. SATB1 defines the developmental context for gene silencing by Xist in lymphoma and embryonic cells. Dev Cell 2009;16:507–16. [PubMed: 19386260]
28. Balamotis MA, Tamberg N, Woo YJ, et al. Satb1 ablation alters temporal expression of immediate early genes and reduces dendritic spine density during postnatal brain development. Mol Cell Biol 2012;32:333–47. [PubMed: 22064485]
29. Fessing MY, Mardaryev AN, Gdula MR, et al. p63 regulates Satb1 to control tissue-specific chromatin remodeling during development of the epidermis. J Cell Biol 2011;194:825–39. [PubMed: 21930775]
30. Han HJ, Russo J, Kohwi Y, Kohwi-Shigematsu T. SATB1 reprogrammes gene expression to promote breast tumour growth and metastasis. Nature 2008;452:187–93. [PubMed: 18337816]
31. Ebralidze AK, Guibal FC, Steidl U, et al. PU.1 expression is modulated by the balance of functional sense and antisense RNAs regulated by a shared cis-regulatory element. Genes Dev 2008;22:2085–92. [PubMed: 18676813]
32. Steidl U, Steidl C, Ebralidze A, et al. A distal single nucleotide polymorphism alters long-range regulation of the PU.1 gene in acute myeloid leukemia. J Clin Invest 2007;117:2611–20. [PubMed: 17694175]
33. Wilkes MC, Siva K, Chen J, et al. Diamond Blackfan anemia is mediated by hyperactive Nemo-like kinase. Nat Commun 2020;11:3344. [PubMed: 32620751]
34. Will B, Vogler TO, Bartholdy B, et al. Satb1 regulates the self-renewal of hematopoietic stem cells by promoting quiescence and repressing differentiation commitment. Nat Immunol 2013;14:437–45. [PubMed: 23563689]
35. Doi Y, Yokota T, Satoh Y, et al. Variable SATB1 levels regulate hematopoietic stem cell heterogeneity with distinct lineage fate. Cell Rep 2018;23:3223–35. [PubMed: 29898394]
36. Satoh Y, Yokota T, Sudo T, et al. The Satb1 protein directs hematopoietic stem cell differentiation toward lymphoid lineages. Immunity 2013;38:1105–15. [PubMed: 23791645]

37. Grosswendt S, Filipchyk A, Manzano M, et al. Unambiguous identification of miRNA:target site interactions by different types of ligation reactions. Mol Cell 2014;54:1042–54. [PubMed: 24857550]
38. Bousquet-Antonelli C, Presutti C, Tollervey D. Identification of a regulated pathway for nuclear pre-mRNA turnover. Cell 2000;102:765–75. [PubMed: 11030620]
39. Yan H, Hale J, Jaffray J, et al. Developmental differences between neonatal and adult human erythropoiesis. Am J Hematol 2018;93:494–503. [PubMed: 29274096]
40. Torkildsen S, Brunetti M, Gorunova L, et al. Rearrangement of the chromatin organizer special AT-rich binding protein 1 gene, SATB1, resulting from a t(3;5)(p24;q14) chromosomal translocation in acute myeloid leukemia. Anticancer Res 2017;37:693–8. [PubMed: 28179318]
41. Karaosmanoglu B, Kursunel MA, Uckan Cetinkaya D, et al. Proerythroblast cells of Diamond–Blackfan anemia patients with RPS19 and CECR1 mutations have similar transcriptomic signature. Front Physiol 2021;12:679919. [PubMed: 34177624]
42. Matsumoto K, Isagawa T, Nishimura T, et al. Stepwise development of hematopoietic stem cells from embryonic stem cells. PLoS One 2009;4: e4820. [PubMed: 19287487]
43. Aspesi A, Monteleone V, Betti M, et al. Lymphoblastoid cell lines from Diamond Blackfan anaemia patients exhibit a full ribosomal stress phenotype that is rescued by gene therapy. Sci Rep 2017;7:12010. [PubMed: 28931864]
44. Hattori H, Janky R, Nietfeld W, Aerts S, Madan Babu M, Venkitaraman AR. p53 shapes genome-wide and cell type-specific changes in micro-RNA expression during the human DNA damage response. Cell Cycle 2014;13:2572–86. [PubMed: 25486198]
45. Laudato S, Patil N, Abba ML, et al. P53-induced miR-30e-5p inhibits colorectal cancer invasion and metastasis by targeting ITGA6 and ITGB1. Int J Cancer 2017;141:1879–90. [PubMed: 28656629]
46. Raut SK, Singh GB, Rastogi B, et al. miR-30c and miR-181a synergistically modulate p53–p21 pathway in diabetes induced cardiac hypertrophy. Mol Cell Biochem 2016;417:191–203. [PubMed: 27221738]
47. Wang J, Jiao Y, Cui L, Jiang L. miR-30 functions as an oncomiR in gastric cancer cells through regulation of P53-mediated mitochondrial apoptotic pathway. Biosci Biotechnol Biochem 2017;81:119–26. [PubMed: 27729002]
48. Pereboom TC, Bondt A, Pallaki P, et al. Translation of branched-chain aminotransferase-1 transcripts is impaired in cells haploinsufficient for ribosomal protein genes. Exp Hematol 2014;42:394–403. e394. [PubMed: 24463277]
49. Moniz H, Gastou M, Leblanc T, et al. Primary hematopoietic cells from DBA patients with mutations in RPL11 and RPS19 genes exhibit distinct erythroid phenotype in vitro. Cell Death Dis 2012;3:e356. [PubMed: 22833095]
50. Noh JY, Gandre-Babbe S, Wang Y, et al. Inducible Gata1 suppression expands megakaryocyte-erythroid progenitors from embryonic stem cells. J Clin Invest 2015;125:2369–74. [PubMed: 25961454]
51. Ashley RJ, Yan H, Wang N, et al. Steroid-resistance in Diamond Blackfan anemia associates with p57Kip2 dysregulation in erythroid progenitors. J Clin Invest 2020;130:2097–110. [PubMed: 31961825]
52. Marinkovic D, Zhang X, Yalcin S, et al. Foxo3 is required for the regulation of oxidative stress in erythropoiesis. J Clin Invest 2007;117:2133–44. [PubMed: 17671650]
53. Han S, Xia J, Qin X, Han S, Wu A. Phosphorylated SATB1 is associated with the progression and prognosis of glioma. Cell Death Dis 2013;4:e901. [PubMed: 24176859]
54. Kumar PP, Purbey PK, Ravi DS, Mitra D, Galande S. Displacement of SATB1-bound histone deacetylase 1 corepressor by the human immuno-deficiency virus type 1 transactivator induces expression of interleukin-2 and its receptor in T cells. Mol Cell Biol 2005;25:1620–33. [PubMed: 15713622]
55. Lee JJ, Kim M, Kim HP. Epigenetic regulation of long noncoding RNA UCA1 by SATB1 in breast cancer. BMB Rep 2016;49:578–83. [PubMed: 27697109]

HIGHLIGHTS

- Chromatin-binding protein, SATB1, is downregulated in differentiating DBA erythroblasts.
- SATB1 is required to induce chromatin loops surrounding the HSP70 gene loci that regulate GATA1.
- SATB1-Dependent induction of HSP70 is required for MEP and megakaryocyte expansion.
- This work increases our understanding of SATB1 in normal human hematopoiesis and DBA pathogenesis.

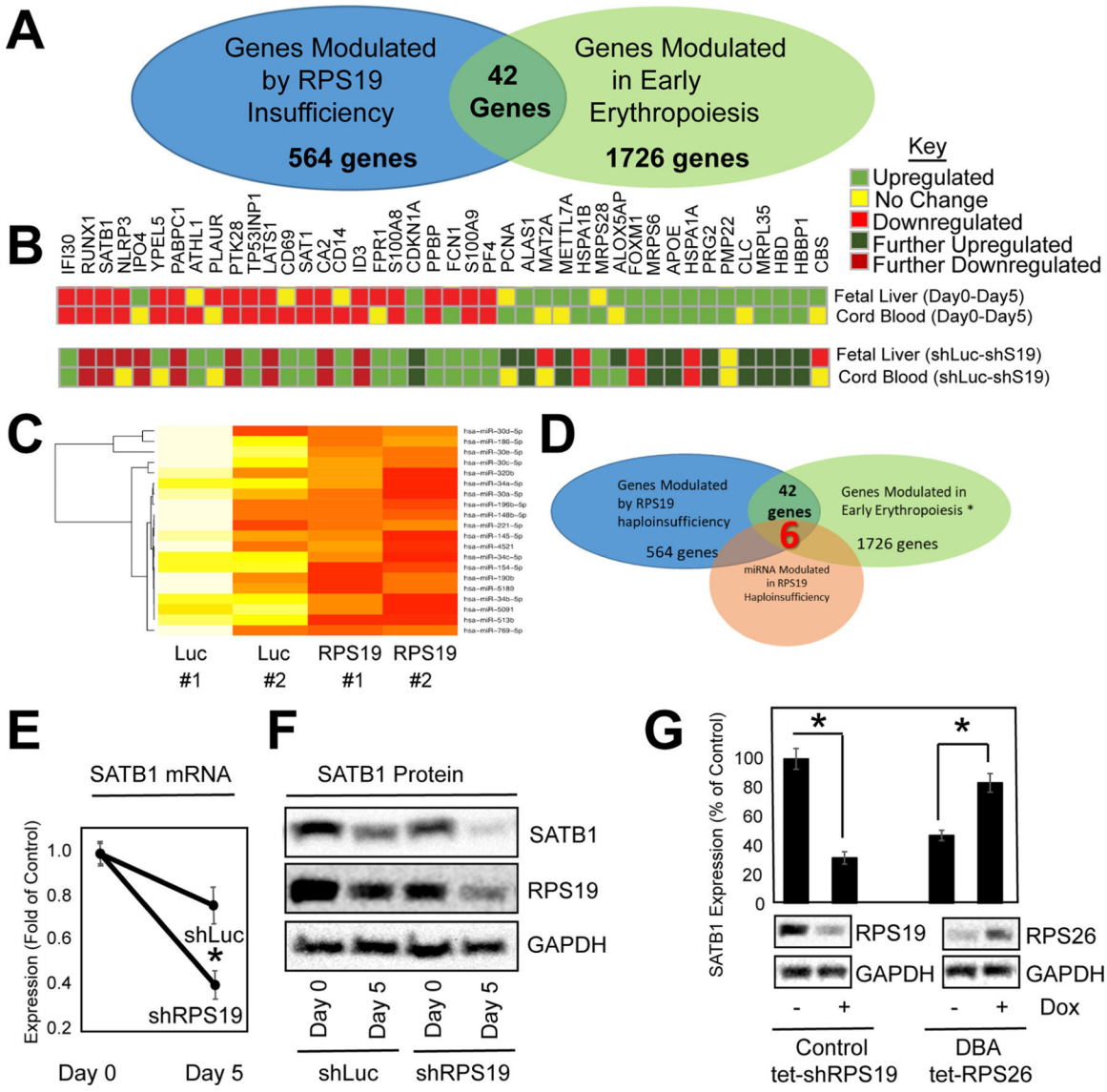

Figure 1.

Deregulated SATB1 identified as master regulator of RPS19-sensitive early erythroid genes. (**A**) RNA transcripts differentially regulated by RPS19 insufficiency in differentiating fetal liver-derived hematopoietic stem and progenitor cells (HSPCs) were cross referenced with RNA transcripts differentially expressed between cord blood-derived $CD34^+$ HSPCs and early burst-forming unit–erythroid (BFU-E) progenitors. Data sets are represented diagrammatically, with differentially regulated transcripts from one data set designated in *blue*, the other data set in *green*. Forty-two transcripts are found in both data sets, represented by the overlapping region, and are designated RPS19-sensitive early erythroid genes. (**B**) $CD34^+$ HSPC cord blood or fetal liver were transduced with shRNA against luciferase and differentiated for 0 or 5 days in erythroid-promoting medium, and expression of RPS19-sensitive early erythroid genes was determined by quantitative reverse transcription polymerase chain reaction (qRT-PCR). Upregulation is denoted in *green* while downregulation is in *red*. $CD34^+$ HSPCs transduced and comparatively designated

as upregulated (*green*), further upregulated (*dark green*), downregulated (*red*), or further downregulated (*dark red*). No deregulation is depicted in *yellow*. (**C**) miRNA-seq was performed comparing fetal liver HSPCs transduced with control (shLuc) or shRNA against RPS19 (shRPS19). Upregulated miRNAs are represented in darker shades of *orange/red*. (**D**) The 3′-untranslated region (3′UTR) sequences of RPS19-senstive early erythroid genes were screened for consensus sequences for the two most highly RPS19-deregulated miRNAs, identifying six transcripts. Expression of (**E**) SATB1 mRNA and (**F**) protein was analyzed at days 0 and 5 in fetal liver-derived differentiating HSPCs by qRT-PCR (n = 5) (**E**) and Western blot analysis (n = 3, representative image shown) (**F**), respectively. Cells were left untransduced or were transduced with shRNA against luciferase or RPS19. Data are represented as means ± SD. (**G**) iPSCs clones were generated from mononuclear cells from bone marrow aspirates from a healthy control and RPS26 mutation-bearing DBA patient. iPSCs were differentiated to $CD34^+$ iHSCs through wnt stimulation. Three iHSC clones (n = 3) for each group were transduced with tetracycline-inducible shRNA against RPS19 or cDNA for RPS26. After 5 days of differentiation, cultures were lysed and SATB1 mRNA was assessed by qRT-PCR. Data are displayed as means ± SD. *Two-tailed Student t test significant at $p < 0.05$. See also Supplementary Figure E1 (online only, available at www.exphem.org).

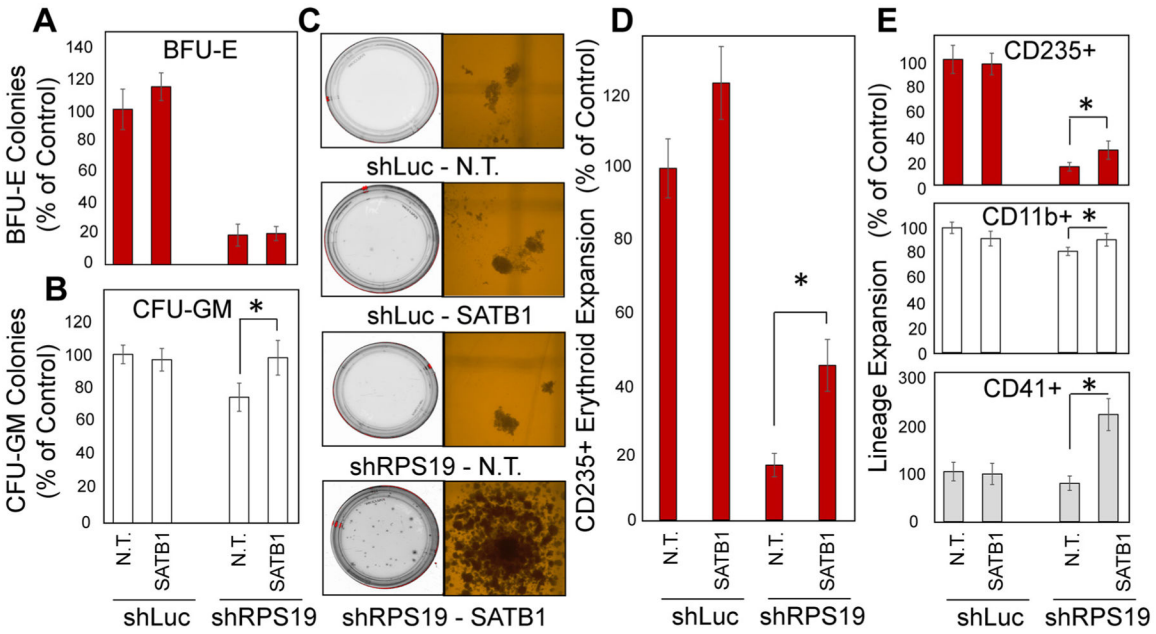

Figure 2.

SATB1 re-expression modestly increases erythroid expansion but increases megakaryocyte and other myeloid lineages. CB CD34$^+$ hematopoietic stem and progenitor cells (HSPCs) were transduced with shRNA against RPS19 in the presence or absence of SATB1 cDNA and plated in methylcellulose containing hematopoiesis-promoting medium ($n = 5$). Resulting burst-forming unit–erythroid (BFU-E) (**A**) and colony-forming unit–granulocyte/macrophage (CFU-GM) colonies (**B**) were scored. Representative images of plates are shown (**C**, left) along with representative BFU-E colonies (**C**, right). Bar = 200 μm. (**D**) Methylcellulose was dissolved in 4°C water, and cell number assessed by hemacytometer. The proportion of CD235$^+$ cells was assessed, and the number of CD235$^+$ cells was calculated by dividing the number of totals cells by the percentage of CD235$^+$. Values are expressed as a fold of control to normalize for experimental variability. (**E**) CB CD34$^+$ HSPCs ($n = 3$) were transduced with shRNA against RPS19 in the presence or absence of SATB1 cDNA and grown in liquid culture for 12 days before flow cytometry and calculation of CD235$^+$, CD11b$^+$, and CD41a$^+$ populations. Data are represented as means ± SD. *Two-tailed Student *t*-test significant at $p < 0.05$. See also Supplementary Figure E2 (online only, available at www.exphem.org).

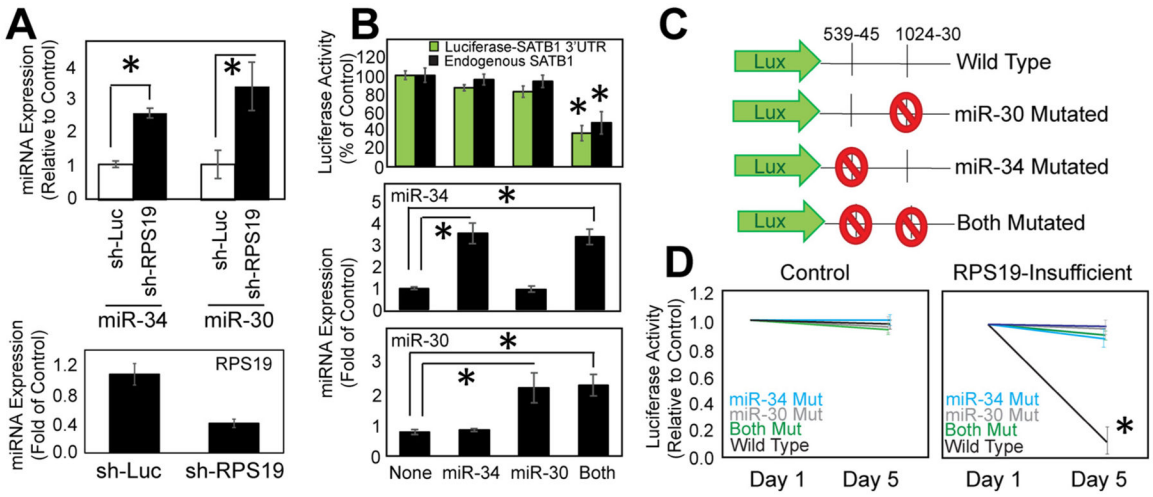

Figure 3.

Premature downregulation of SATB1 in erythroid progenitors requires miR-30 and miR-34. (**A**) $CD34^+$ hematopoietic stem and progenitor cells (HSPCs) co-expressing shRNA against a nontargeting sequence or RPS19 were differentiated for 5 days in erythropoiesis-promoting medium, and expression of miR-30 and miR-34 (upper panel) and RPS19 (lower panel) was determined by quantitative reverse transcription polymerase chain reaction (qRT-PCR) ($n = 3$). (**B**) FL $CD34^+$ cells were transduced with mimetics of miR-30, miR-34, or both, along with SATB1 3′ untranslated region (UTR)-luciferase. Luciferase activity was assessed at day 5, before cell lysis and qRT-PCR analysis of endogenous SATB1 protein ($n = 3$ in duplicate). In the upper panel, *green bars* indicate luciferase activity, while the *black* bars represent endogenous SATB1 expression. (**C**) The wild-type 3′UTR of SATB1, along with 3′UTR containing mutations in miR-30, miR-34, or both consensus binding sequences were fused to the luciferase gene. (**D**) SATB1 3′UTR-luciferase constructs were transduced into fetal liver (FL) $CD34^+$ HSPCs co-expressing shRNA against a nontargeting sequence (left) or RPS19 (right). Luciferase activity was assessed at days 1 and 5 ($n = 3$ in duplicate). Data are represented as means. *Two-tailed Student *t* test, significant at $p < 0.05$. See also Supplementary Figure E3 (online only, available at www.exphem.org).

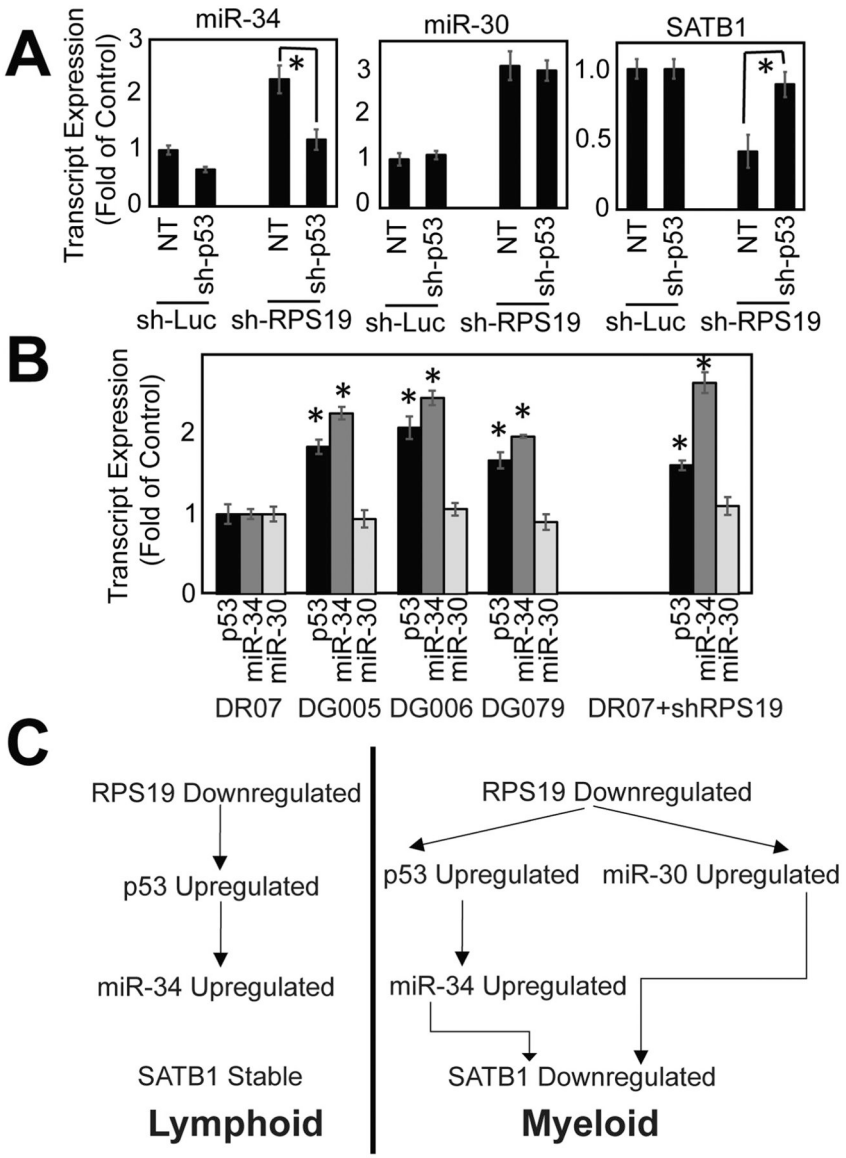

Figure 4.

Induction of miR-34 in RPS19 insufficiency is p53 dependent. (**A**) CB CD34^{+} hematopoietic stem and progenitor cells (HSPCs) were transduced in erythropoiesis-promoting medium with shRNA against luciferase or RPS19 and nontargeting or p53 before miR-30, miR-34, and SATB1 analysis by quantitative reverse transcription polymerase chain reaction (qRT-PCR) at day 5 ($n = 3$). (**B**) Lymphoblastic cell lines derived from DBA patients were assessed for miR-30 and miR-34 by qRT-PCR. These were compared with a lymphoblastic cell line derived from a healthy control, or the same control transduced with shRNA against RPS19. Significance is indicated (*) when expression is greater ($p \leq 0.05$) than observed in the corresponding DR07 control ($n = 7$). (**C**) Diagrammatic representation of the proposed myeloid lineage-specific premature downregulation of SATB1. In lymphoblastic cells, RPS19 insufficiency induces miR-34 through p53 but this is insufficient to downregulate SATB1. In myeloid lineage cells, RPS19 insufficiency induces both miR-30 and miR-34,

which synchronize to prematurely downregulate SATB1. Data are represented as means ± SD. *Two-tailed Student *t* test significant at $p < 0.05$. See also Supplementary Figure E4 (online only, available at www.exphem.org).

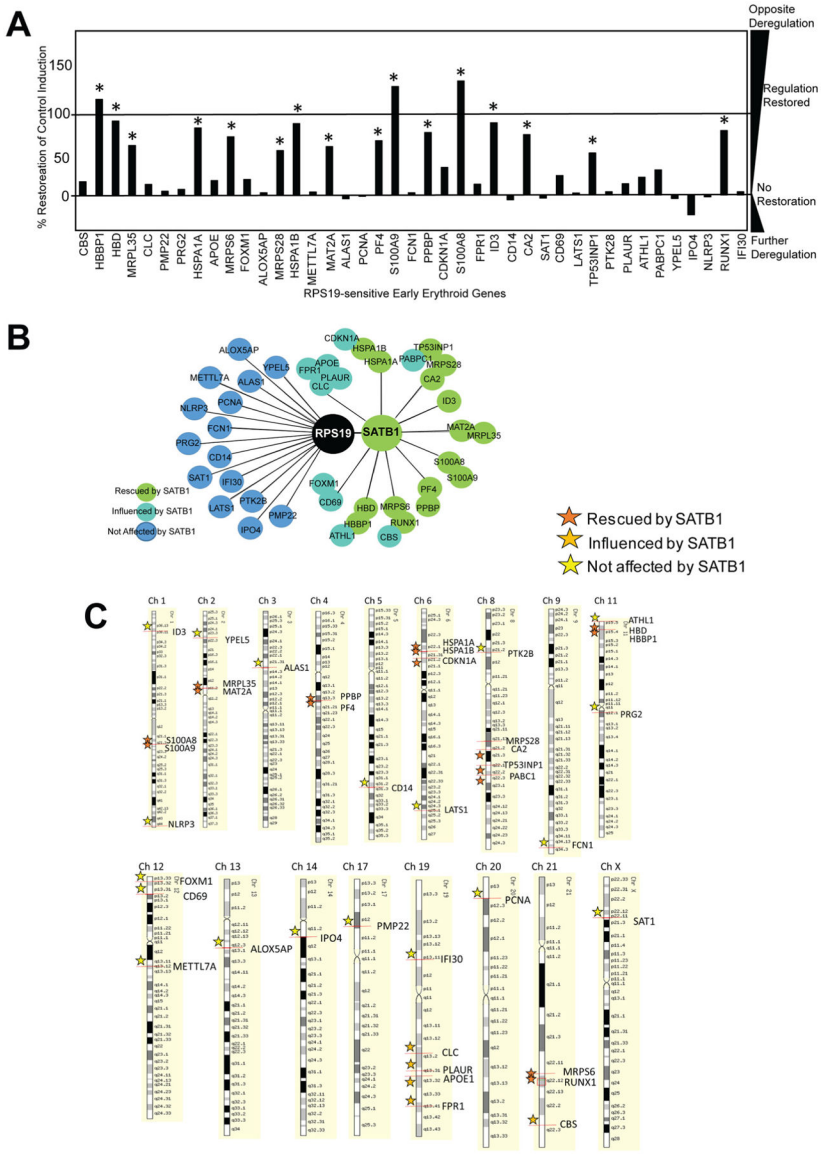

Figure 5.

SATB1 required for appropriate regulation of 16 RPS19-sensitive early erythroid genes. (**A**) Cord blood CD34^{+} hematopoietic stem and progenitor cells (HSPCs) were transduced with shRNA against RPS19 in erythropoiesis-promoting medium in the presence or absence of recombinant SATB1 ($n = 3$). After 5 days, reverse transcription polymerase chain reaction (qRT-PCR) was performed on 42 RPS19-sensitive early erythroid genes. Values were compared with expected values from healthy controls, with 0% representing no rescue, and 100% correlating to values restored to the healthy state. Data are represented as means ± SD. *Two-tailed Student *t* test, significant at $p < 0.05$. (**B**) Diagrammatic representation of regulation of RPS19-sensitive genes by SATB1. Genes are grouped by chromosome location regulation. Gene regulation largely restored (>50%) by SATB1 is represented in *green*, somewhat restored (<50%) in *teal*, and those not influenced in *blue*. (**C**) Gene loci on chromosomes of RPS19-sensitive genes are diagrammatically presented with SATB1-

responsive genes in *orange* and SATB1-independent genes in *yellow*. See also Figure E5 (online only, available at www.exphem.org).

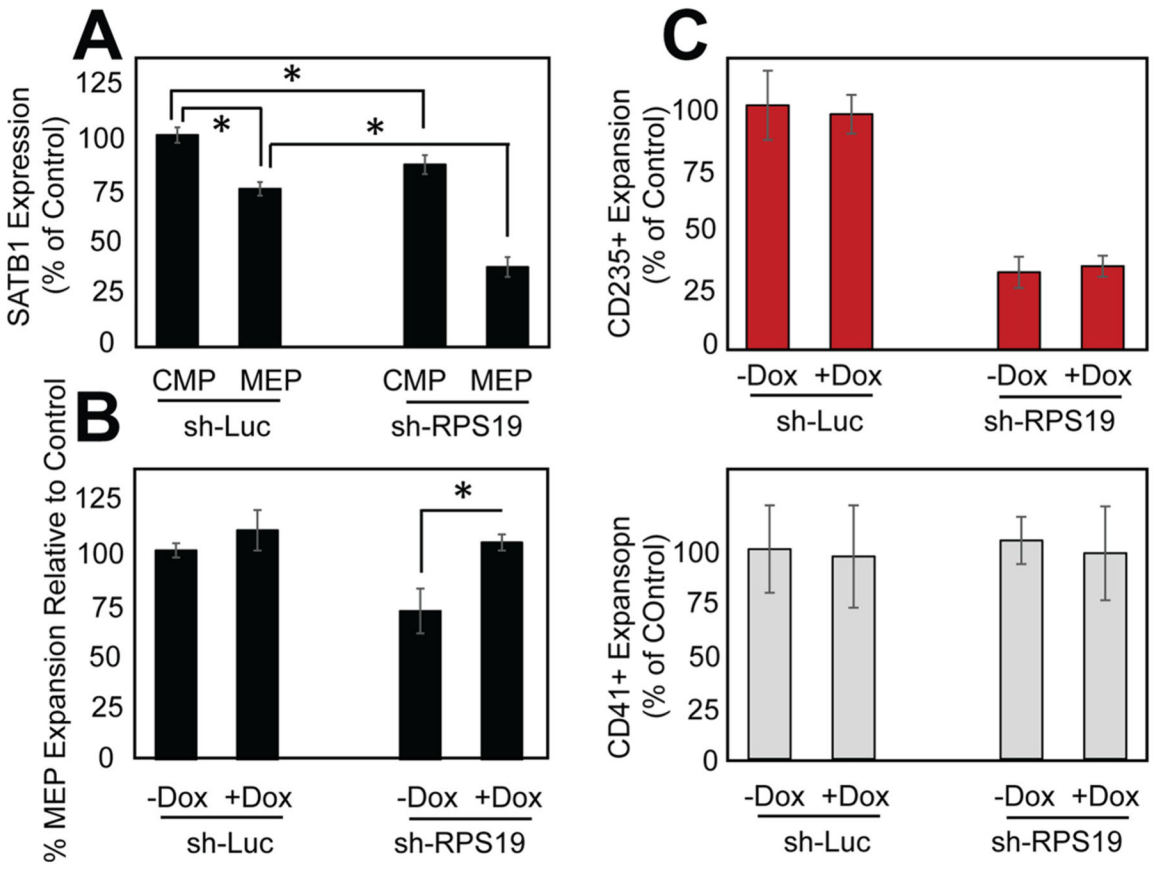

Figure 6.

SATB1 re-expression rescues megakaryocyte/erythroid progenitor (MEP) expansion but does not correct erythropoiesis in RPS19 insufficiency. (**A**) Cord blood $CD34^+$ hematopoietic stem and progenitor cells (HSPCs) were transduced with shRNA against RPS19 or Luc and cultured for 4 days in hematopoiesis-promoting medium. Cells were sorted for Lin^-CD34^+ $CD38^{mid}CD45RA^-FLT3^-MPL^+CD36^-CD41^-$ MEPs and $CD34^+CD38^+CD45RA^-FLT3^+MPL^+CD36^-CD41^-$ common myeloid progenitors (CMPs) by fluorescence-activated cell sorting (FACS), and SATB1 expression was analyzed by reverse transcription polymerase chain reaction (qRT-PCR). (**B**) CB $CD34^+$ HSPCs were sorted for $CD34^+CD38^+CD45RA^-FLT3^+MPL^+CD36^-CD41^3$ CMPs by FACs and transduced with shRNA against RPS19 and tetracycline-inducible SATB1. After 4 days of differentiation in hematopoiesis-promoting medium, $Lin^-CD34^+CD38^{mid}$ $CD45RA^-FLT3^-MPL^+CD36^-CD41^-$ MEPs were assessed by flow cytometry. Representative gating and validation of $CD235^+$ erythroid and $CD41^+$ megakaryocyte differentiation is presented in Supplementary Figure E6 (online only, available at www.exphem). (**C**) $Lin^-CD34^+CD38^{mid}$ $CD45RA^-FLT3^-MPL^+CD36^-CD41^-$ MEPs were enriched from cord blood $CD34^+$ HSPCs and transduced with shRNA against RPS19 and tetracycline-inducible SATB1. After 10 days of differentiation, $CD235^+$ erythroid and $CD41^+$ megakaryocyte expansion was determined. Experiments were performed in triplicate and repeated a minimum of three times. Data are represented as means ± SD, and significance is defined at $p < 0.05$.

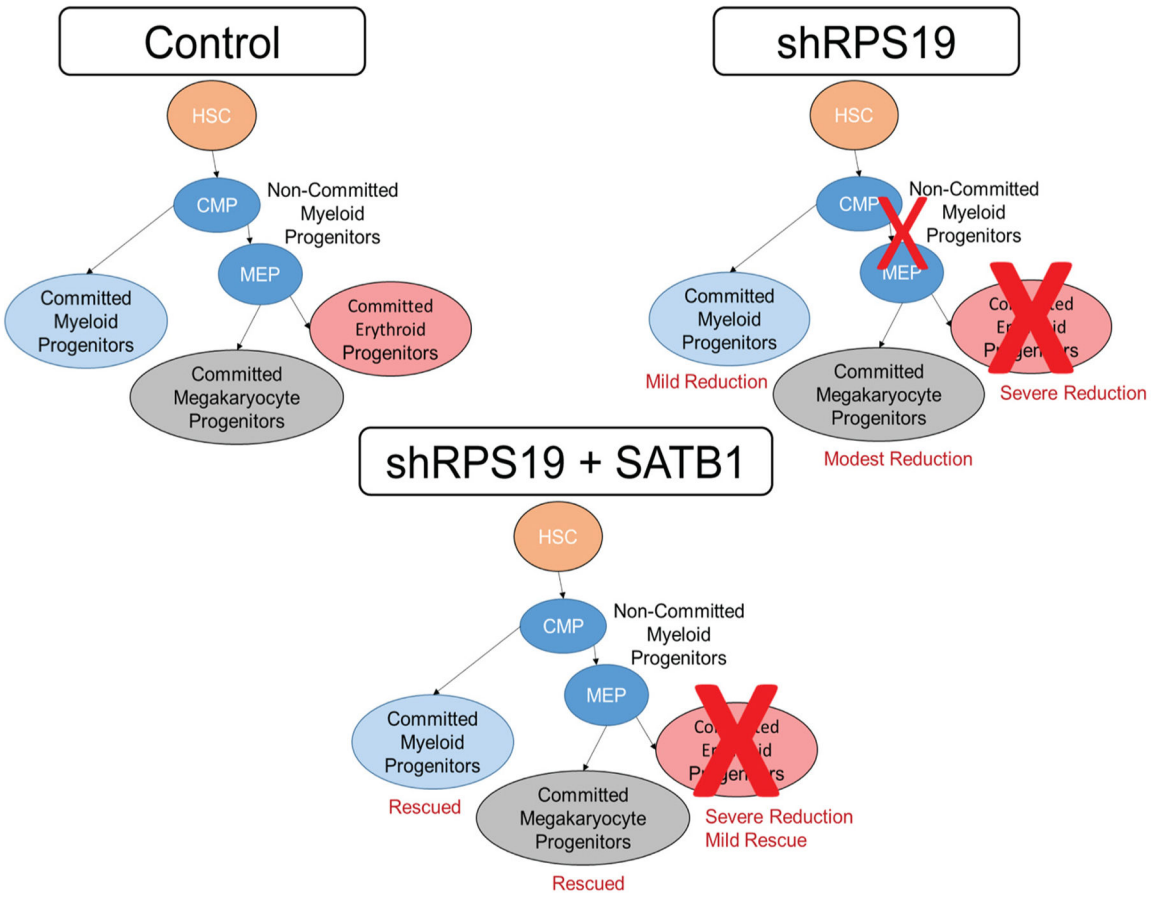

Figure 7.

In RPS19 insufficiency, re-expression of SATB1 rescues defects in noncommitted progenitor populations without affecting committed erythroblast defects. Schematics of hematopoiesis indicating stages of differentiation (**A**) and stages affected by RPS19 insufficiency (**B**). Re-expression of SATB1 significantly corrects defects in noncommitted erythropoiesis but the later defect is SATB1 independent (**C**).